Nuclear Physics B142 (1978) 344–364

DOUBLE REGGE EXCHANGE PHENOMENOLOGY

T. SHIMADA and A.D. MARTIN
Department of Physics, Durham University, UK

A.C. IRVING
DAMTP, Liverpool University, UK

Received 3 July 1978

We construct a double Regge exchange amplitude which has the proper analytic structure and which is phenomenologically viable. The various couplings involved can be estimated using pole extrapolation techniques which are successful in two-body scattering. We explicitly calculate the double Regge exchange contributions to the well-measured, and related, processes $K^{\pm}p \to K^0\pi^{\pm}p$ and $\pi^-p \to K^-K^0p$. In this way the observed features of the dimeson partial-wave production amplitudes are used to test the double-exchange approach.

1. Introduction

Multi-Regge theory has played an important rôle in theoretical studies of multiparticle hadronic interactions [1,2]. However, its phenomenological validity has not yet been subjected to the same level of scrutiny as has Regge theory in two-body scattering [3,4]. In this paper, we shall set up a double Regge exchange amplitude for the dimeson production reactions $0^-\,\frac{1}{2}^+ \to 0^-0^-\,\frac{1}{2}^+$, where the parameters can be completely determined from two-body scattering, and confront it with high-statistics data.

Considerable use has been made of the double Regge exchange amplitude for describing inelastic diffraction, for example the reggeised pion exchange Deck amplitude [5]. In such applications the production amplitude phase is often difficult to observe experimentally and is usually assumed to be given by the product of the two Regge signature factors. Strictly speaking, this last assumption is incorrect, since, in order to satisfy analyticity requirements, the reggeon-reggeon-particle vertex must also carry a non-trivial phase. By interfering our model amplitude with well-known resonance production amplitudes, we may investigate this subtle, but important, feature of multi-Regge amplitudes.

To our knowledge, this is the first attempt to predict the overall magnitude of a multi-Regge amplitude *. The fact that such off-shell extrapolations work for the couplings in two-body scattering [6,4] is an important dynamical feature of hadronic processes, and encourages a similar test for $2 \to 3$ body scattering. Of course, this is as much a test of the precise t-dependent extrapolation functions (Regge residues) as of Regge pole behaviour itself ($\sim s^{\alpha(t)}$). In the $2 \to 2$ case the Regge residues predicted by the B_4 dual amplitude give satisfactory results [4]. Here, in the $2 \to 3$ case, we shall use the analogous residues predicted by the B_5 dual amplitude [7].

The reactions

$$K^- p \to \bar{K}^0 \pi^- p \,, \tag{1a}$$

$$K^+ p \to K^0 \pi^+ p \,, \tag{1b}$$

$$\pi^- p \to K^- K^0 p \,, \tag{2a}$$

$$\pi^+ p \to K^+ K^0 p \,, \tag{2b}$$

provide a convenient framework within which to investigate double Regge exchange. First, the double-exchange contributions to these processes are closely interrelated. Moreover, high-statistics data have recently been obtained for the first three processes, with the dimeson system scattered into the forward direction [8–11]. Thus, not only can we compare the double-exchange predictions with the data for an individual reaction, but we can make a more extensive investigation by comparing the agreement for a set of related reactions.

Not only are the reggeon couplings to the external particles in processes 1 and 2 well-known, but the reggeon-reggeon-particle couplings at the middle vertex can be related to equally well-known coupling constants. A further advantageous feature of these processes is that all final state particles are stable so that there are no rescattering corrections to complicate the interpretation of phases, as, for example, they do in $\pi N \to \pi\rho N \to \pi\pi\pi N$.

The reactions of 1 and 2 are analogous to $K^\pm p$ and $\pi^\pm p$ elastic scattering respectively; the sum of the cross sections for each pair measures the strength of the pomeron exchange component, while the difference measures the odd charge conjugation (ω and ρ) exchange contribution. Our knowledge of the pomeron in inelastic resonance production has recently been improved [12,13]. We shall pay some attention to its rôle in processes 1 and 2, with particular reference to the powerful f dominated pomeron scheme [14].

Ideally, one would like to compare the double Regge amplitude with high-energy data in which both 0^-0^- and $0^- \frac{1}{2}^+$ sub-energies were large. However, most high-statistics spectrometer data are at relatively low 0^-0^- effective mass. This is not such a disadvantage in practice, since the prominent resonance production amplitudes in this region can be used as well-measured and well-understood reference

* Although the reggeised Deck model is absolutely normalised, this is not a strong test, since the π exchange is not far off-shell.

waves with which to interfere the 0^-0^- partial waves thought to be due to double Regge exchange. This present investigation was, in part, motivated by the observation [9] of anomalous partial-wave behaviour in processes 1.

The organisation of the paper is as follows. In sect. 2 we construct a double Regge exchange amplitude, which has the proper analytic structure, and which can be explicitly evaluated for the dimeson production reactions under study. We describe how to determine the required Regge vertices from well-known couplings and we show how all the relevant double-exchange contributions are related one to another. We also discuss the inclusion of the pomeron. The comparison with the data is made in sect. 3. To be specific, it is the observed structures of the dimeson partial-wave amplitudes, which have been extracted [9,11] from the data, with which we confront the double exchange model. Our conclusions are given in sect. 4.

2. Structure of the amplitudes

In this section we describe the explicit form used to calculate the $Kp \to K\pi p$ and $\pi p \to K\bar{K}p$ amplitudes. We describe the structure of the two-reggeon exchange contributions, and how the various couplings are determined. Then we discuss the model used to calculate the reggeon-pomeron contributions.

2.1. Double Regge limit

We wish to calculate the amplitude for a process of the type $ab \to 123$ shown in fig. 1. For simplicity we first consider scalar external particles. The double Regge limit of the amplitude corresponds to s_1, s_2, $s \to \infty$ and $\eta \equiv s/(\alpha' s_1 s_2)$, t_1, t_2 fixed.

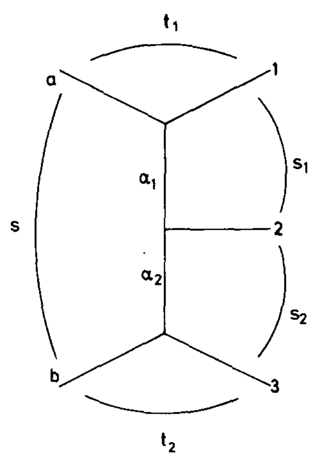

Fig. 1. Kinematic variables for the process $ab \to 123$.

The requirement that the amplitude is free of simultaneous discontinuities in two overlapping channel invariants leads to the general form [1]

$$T = \Gamma(-\alpha_1)\,\Gamma(-\alpha_2)[(-\alpha' s)^{\alpha_1}(-\alpha' s_2)^{\alpha_2-\alpha_1}\,V_1(\eta, t_1, t_2) + (-\alpha' s)^{\alpha_2}(-\alpha' s_1)^{\alpha_1-\alpha_2}\,V_2(\eta, t_1, t_2)]\,, \tag{3}$$

where the reggeon-reggeon-particle vertex functions, V_i, are regular functions of η. The general form for the V_i follows from the Mellin representation for the signatured amplitude [1]

$$T^{\tau_1\tau_2} = \left(\frac{1}{2\pi i}\right)^3 \int \mathrm{d}\lambda \int \mathrm{d}J_1 \int \mathrm{d}J_2\,\Gamma(-\lambda)\,\Gamma(-J_1+\lambda)\,\Gamma(-J_2+\lambda)(-\alpha' s_1)^{J_1-\lambda} \times (-\alpha' s_2)^{J_2-\lambda}(-\alpha' s)^{\lambda} a^{\tau_1\tau_2}(J_1, J_2, \lambda; t_1, t_2)\,. \tag{4}$$

If the partial-wave amplitude has a dominant double Regge pole singularity,

$$a^{\tau_1\tau_2} \approx \frac{\beta(\lambda, t_1, t_2)}{(J_1-\alpha_1)(J_2-\alpha_2)}\,, \tag{5}$$

then moving the J_i contours, and collecting the residues of these poles, we find, as $s_1, s_2 \to \infty$

$$T^{\tau_1\tau_2} \sim \frac{1}{2\pi i} \int \mathrm{d}\lambda\,\Gamma(-\lambda)\,\Gamma(-\alpha_1+\lambda)\,\Gamma(-\alpha_2+\lambda)(-\alpha' s_1)^{\alpha_1-\lambda} \times (-\alpha' s_2)^{\alpha_2-\lambda}(-\alpha' s)^{\lambda}\beta(\lambda, t_1, t_2)\,.$$

Now on closing the helicity contour to the left, and picking up the helicity poles in the last two Γ functions, we obtain

$$V_1(\eta, t_1, t_2) = \frac{1}{\Gamma(-\alpha_1)\,\Gamma(-\alpha_2)} \sum_{n=0}^{\infty} \frac{1}{n!}\,\Gamma(-\alpha_1+n)\,\Gamma(-\alpha_2+\alpha_1-n)\,\eta^{-n} \times \beta(\alpha_1-n, t_1, t_2)\,, \tag{6}$$

with an identical expression for V_2 except that $\alpha_1 \leftrightarrow \alpha_2$. The minimal choice for the residue, $\beta(\lambda, t_1, t_2) = \beta_0$ with β_0 independent of λ, thus leads to the concise parametrization

$$V_1 = \beta_0\,\frac{\Gamma(\alpha_1-\alpha_2)}{\Gamma(-\alpha_2)}\;{}_1F_1\!\left(-\alpha_1, 1-\alpha_1+\alpha_2, -\frac{1}{\eta}\right) \tag{7}$$

and $V_2 = V_1(\alpha_1 \leftrightarrow \alpha_2)$. This agrees with the double Regge limit of the scalar dual amplitude [7].

We are concerned with a process ab $\to$ 123 in which three of the external particles are pseudoscalar. In this case the above representation applies to the kinematical singularity free amplitude $\hat{T}$ defined by

$$T = K\hat{T}\,, \tag{8}$$

with

$$\begin{aligned} K &= \epsilon_{\alpha\beta\gamma\delta}\,(p_3 - p_b)^\alpha (p_3 + p_b)^\beta (p_a - p_1)^\gamma (p_a + p_1)^\delta \\ &= -4Mp_a p_3 p_1 \sin\chi \sin\theta_1 \sin\phi_1\,, \end{aligned} \tag{9}$$

where $\chi(s, t_2)$ is the crossing angle between the s and t channel helicity frames for the quasi-two-body process ab $\to$ (12)3; θ_1 and ϕ_1 specify the decay angles in the (12) rest frame and M is the mass of the (12) system.

The dynamics of the reactions are controlled by $\hat{T}$. However, at low masses (M) the angular variations observed in $|T|^2$ come mainly from the kinematical factor K of eq. (8). This is because $\hat{T}$ is dominated by low partial waves * and because, in any case, phase space limits the range across which $\hat{T}$ may vary. At low mass or energy, therefore, a comparison of $|T|^2$ with the experimental distributions may simply check the K factor [15]. On the other hand, if we compare $K^\pm$ initiated reactions (i.e. the difference between related amplitudes at the same point in phase space), or study partial-wave phases, we shall probe the dynamics ($\hat{T}$) rather than the trivial kinematic function K.

In the double Regge limit $|K| \sim \eta s_1 s_2$, and this implies

$$\hat{T} \sim s_1^{\alpha_1 - 1} s_2^{\alpha_2 - 1}\,. \tag{10}$$

Further, we consider Regge trajectories α_1, α_2 with lowest (exchange-degenerate) particle spin 1. To obtain the form of $\hat{T}$ we therefore need to make the replacements $\alpha_i \to \alpha_i - 1$. That is, eq. (3) becomes

$$\begin{aligned} T = K\Gamma(1-\alpha_1)\,\Gamma(1-\alpha_2)[&(-\alpha' s)^{\alpha_1 - 1}(-\alpha' s_2)^{\alpha_2 - \alpha_1}\hat{V}_1 \\ &+ (-\alpha' s)^{\alpha_2 - 1}(-\alpha' s_1)^{\alpha_1 - \alpha_2}\hat{V}_2]\,, \end{aligned} \tag{11}$$

with (cf. eq. (7))

$$\hat{V}_1(\eta, t_1, t_2) = \beta_0\,\frac{\Gamma(\alpha_1 - \alpha_2)}{\Gamma(1-\alpha_2)}\;{}_1F_1\!\left(1-\alpha_1, 1-\alpha_1+\alpha_2, -\frac{1}{\eta}\right). \tag{12}$$

Using eq. (11) to construct signatured amplitudes we obtain [1]

$$\begin{aligned} T^{\tau_1\tau_2} = &-K\Gamma(1-\alpha_1)\,\Gamma(1-\alpha_2) \\ &\times [(\alpha' s)^{\alpha_1 - 1}(\alpha' s_2)^{\alpha_2-\alpha_1}\xi_1\xi_{21}\hat{V}_1 + (\alpha' s)^{\alpha_2 - 1}(\alpha' s_1)^{\alpha_1 - \alpha_2}\xi_2\xi_{12}\hat{V}_2]\,, \end{aligned} \tag{13}$$

* Since $K \propto \sin\theta_1 \sin\phi_1 \propto Y_1^1(\theta_1, \phi_1) + Y_1^{-1}(\theta_1, \phi_1)$, P wave dominance of T corresponds to $\hat{T} \sim$ const.

where the signature factors are

$$\xi_i = \tfrac{1}{2}(\tau_i + \mathrm{e}^{-i\pi\alpha_i}) ,$$

$$\xi_{ij} = \tfrac{1}{2}(\tau_i\tau_j + \mathrm{e}^{-i\pi(\alpha_i-\alpha_j)}) .$$

Note that, in a numerical evaluation of the amplitude, care is needed as the vertex functions contain "spurious" poles. These arise from $\Gamma(\alpha_1 - \alpha_2)$ in $\hat{V}_1$ and $\Gamma(\alpha_2 - \alpha_1)$ in $\hat{V}_2$ whenever $\alpha_i - \alpha_j$ takes non-positive integral values with α_1, α_2 non-integer. These poles cancel in the expression for the amplitude. For example, with the minimal choice of residue, $\beta(\lambda; t_1, t_2) = \beta_0$ independent of λ, the poles arising from $\Gamma(\alpha_1 - \alpha_2)$ of $\hat{V}_1$ cancel with the poles arising from ${}_1F_1(\cdots, 1 - \alpha_2 + \alpha_1, ...)$ of $\hat{V}_2$.

A cruder approximation than $\beta = \beta_0$ is to include only a single term ($n = 0$) in the infinite series for the $\hat{V}_i$ functions, provided $\eta \gg 1$. In this case the above cancellation mechanism is destroyed, and only the first "spurious" pole (corresponding to $\alpha_1 - \alpha_2 = 0$) is killed. We must then only include the first pole in $\Gamma(\alpha_i - \alpha_j)$ by making the approximation $\Gamma(\alpha_i - \alpha_j) \approx 1/(\alpha_i - \alpha_j)$. This two-stage approximation is the procedure adopted in the analysis of Berger and Vergeest [16].

However to study the partial-wave amplitudes of the (12) system we require the amplitude over the whole kinematically allowed s_2 and t_1 region for fixed values of s, t_2 and $s_1 \equiv M^2$. Moreover, in the natural parity-exchange sector which we analyse, we cannot expect such strong peripherality of the amplitude as that arising from π exchange. Indeed the kinematical factor requires the amplitudes to vanish at the boundary ellipse of the kinematical region. We therefore evaluate the full power series, eq. (12), taking care to avoid errors arising from the "spurious" poles.

2.2. Exchanges and coupling structure

The double-exchange amplitudes which we consider for the $\mathrm{Kp} \to \mathrm{K}\pi\mathrm{p}$ reactions are shown in fig. 2. There are two types: those with a fast forward K (type I) and those with a fast forward π (type II). To evaluate a double Regge exchange diagram (ab $\to$ 123) we note that the coupling β_0 appearing in eqs. (12) and (13) is given by the product of two reggeon-particle-particle couplings, $\beta^{1\mathrm{a}}_{\mathrm{R}_1}\beta^{\mathrm{R}_2}_{3\mathrm{b}}$, and one reggeon-reggeon-particle coupling $\gamma_2^{\mathrm{R}_1\mathrm{R}_2}$. The former couplings are accessible from $0^-\frac{1}{2}^+ \to 0^-\frac{1}{2}^+$ scattering. For these we use the simple coupling scheme described in appendix A of ref. [4] which satisfies the constraints of SU(3) * and exchange degeneracy (EXD):

$$T(\mathrm{ab} \to 13) = \beta^{1\mathrm{a}}_{\mathrm{R}}\beta^{\mathrm{R}}_{3\mathrm{b}}\xi_{\mathrm{R}}(\alpha)\,\Gamma(1-\alpha)(\alpha' s)^{\alpha} . \tag{14}$$

This is the Regge limit of a B_4 dual amplitude and is related by factorisation to the

* The only symmetry breaking allowed is in the trajectory functions [17].

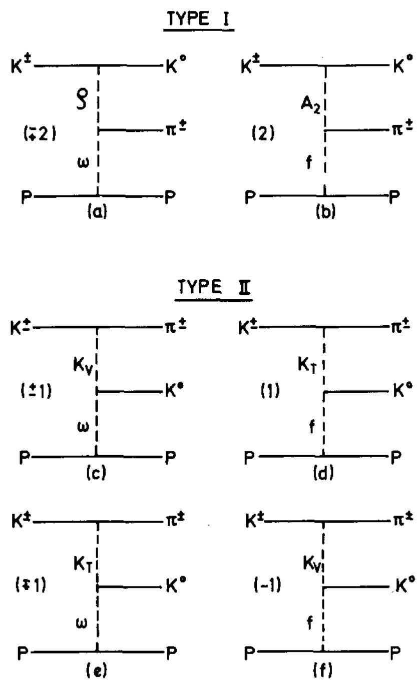

Fig. 2. Double Regge exchange diagrams for the reactions $K^{\pm}p \to K^0\pi^{\pm}p$. The numbers in brackets are the relative weights (see table 1).

analogous double Regge limit of B_5. To demonstrate this we rewrite eq. (13) in the form

$$T(\mathrm{ab} \to 123) = -K\beta^{1a}_{R_1}\xi_1(\alpha_1)\,\Gamma(1-\alpha_1)(\alpha' s_1)^{\alpha_1-1} R_{\tau_1\tau_2}(\alpha_1,\alpha_2) \times \beta^{R_2}_{3b}\,\xi_2(\alpha_2)\,\Gamma(1-\alpha_2)(\alpha' s_2)^{\alpha_2-1}\,, \qquad (15)$$

where

$$R_{\tau_1\tau_2} = \gamma_2^{R_1R_2}\,[\eta^{\alpha_1-1}\xi_2^{-1}\xi_{21}\hat{V}_1 + \eta^{\alpha_2-1}\xi_1^{-1}\xi_{12}\hat{V}_2]/\beta_0\,. \qquad (16)$$

The evaluation of the couplings is effected by pole extrapolation [4]. If $\tau_1 = \tau_2 = -1$, the amplitude of eq. (15) behaves as

$$T(\mathrm{ab} \to 123) \approx \frac{1}{\alpha'^2}\,\beta^{1a}_{R_1}\beta^{R_2}_{3b}\gamma_2^{R_1R_2}K\,\frac{1}{(t_1-m_1^2)(t_2-m_2^2)} \qquad (17)$$

near $\alpha_1(t_1) = 1$, $\alpha_2(t_2) = 1$. Likewise, near $\alpha = 1$, the amplitude of eq. (14) behaves as

$$T(\mathrm{ab} \to 13) \approx \beta^{1a}_{R}\beta^{R}_{3b}\,\frac{s}{t-m_R^2}\,, \qquad (18)$$

so that

$$\frac{T(\mathrm{ab} \to 123)}{T(\mathrm{ab} \to 13)} \approx \frac{\gamma_2^{\mathrm{RR}}}{\alpha'^2} \frac{K}{s} \frac{1}{t - m_{\mathrm{R}}^2} \tag{19}$$

in the simple case where $\mathrm{R}_1 = \mathrm{R}_2 = \mathrm{R}$ (only one type of Regge exchange).

If $g(\mathrm{R}_1\mathrm{R}_2 2)$ is some suitably normalised $1^-1^-0^-$ coupling constant [18], the ratio of the Born-term amplitudes corresponding to eq. (19) is

$$\frac{T^{\mathrm{B}}(\mathrm{ab} \to 123)}{T^{\mathrm{B}}(\mathrm{ab} \to 13)} = g(\mathrm{RR}2) \frac{K}{2s} \frac{1}{t - m_{\mathrm{R}}^2} . \tag{20}$$

Comparing eqs. (19) and (20), we find

$$\gamma_2^{\mathrm{RR}} = \tfrac{1}{2}\, g(\mathrm{RR}2)\, \alpha'^2 . \tag{21}$$

A knowledge of $g(\mathrm{R}_1\mathrm{R}_2 2)$ therefore allows the calculation of the reggeon-reggeon-particle residue $\gamma_2^{\mathrm{R}_1\mathrm{R}_2}$. For this purpose, we choose $g(\omega\rho\pi)$ which may be calculated from $\Gamma_{\omega\to 3\pi}$ using a ρ pole-dominance model [4,18]. We find

$$\gamma_{\pi^-}^{\rho\omega} = 7.1 . \tag{22}$$

We also use [4]

$$\beta_\rho^{\overline{\mathrm{K}}^0\mathrm{K}^-} = -5.7 , \qquad \beta_{\mathrm{pp}}^{\omega} = 8.1 . \tag{23}$$

The values and conventions are those of ref. [4] except that here we use the signature factor $\tau + \mathrm{e}^{-i\pi\alpha}$ rather than $1 + \tau\mathrm{e}^{-i\pi\alpha}$. Notice that the external couplings, such as β_ρ^{KK} and $\beta_{\mathrm{pp}}^{\omega}$, are already known to describe data in the physical region (t_1, $t_2 < 0$). The only untested extrapolation is that used to evaluate the coupling, $\gamma_2^{\mathrm{R}_1\mathrm{R}_2}$, at the middle vertex.

Now using the couplings of eqs. (22) and (23) we may evaluate the contribution of the exchange diagram of fig. 2a. This contribution is given by eqs. (13) and (12) with

$$\beta_0 = \beta_\rho^{\overline{\mathrm{K}}^0\mathrm{K}^-} \gamma_{\pi^-}^{\rho\omega} \beta_{\mathrm{pp}}^{\omega} .$$

To determine the magnitudes and signs of the other diagrams of fig. 2 we apply SU(3) and EXD. To accomplish this we use the elegant quark diagram method developed by Eylon [19]. The quark diagrams are shown in fig. 3 and the corresponding weights are given in table 1. We refer to Eylon [19] for details but some explanatory notes are in order. First, all relevant (connected) quark diagrams are constructed (fig. 3). A given double exchange (α_1, α_2) contributes to all the quark diagrams equally up to a plus or minus sign. The rule to determine the sign is simple: the sign is given by the product of the charge-conjugation eigenvalues of the trajectories corresponding to twisted $\mathrm{q}\overline{\mathrm{q}}$ propagators [19].

The rows of the table give the different (α_1, α_2) contributions which are linked

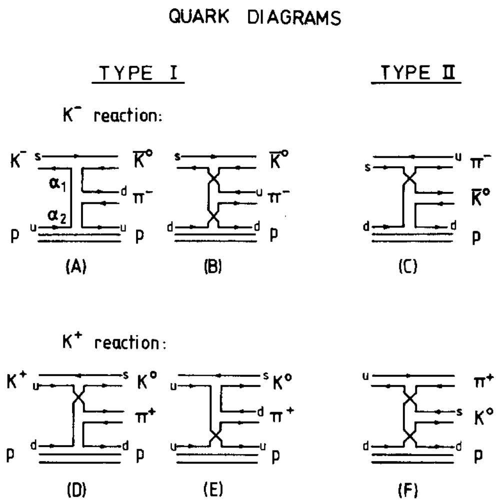

Fig. 3. The quark diagrams for $K^{\pm}p \to K^0\pi^{\pm}p$, required for determining the weights listed in table 1.

by EXD. That is we need to interrelate the four independent types of couplings; TT, VT, TV and VV, where T and V denote tensor and vector exchange. Recall that each of these four amplitudes has the signature structure

$$A_{\alpha_1,\alpha_2} = \tfrac{1}{4}[A + \tau_1 A^{(1)} + \tau_2 A^{(2)} + \tau_1\tau_2 A^{(1,2)}] , \qquad (24)$$

where, for example, $A^{(1)}$ is related to A by the single substitution $s_1 \to -s_1$, and where we have omitted the subscripts α_1, α_2 on the right hand side. It is straightforward to relate the quark topology of the diagrams in fig. 3 to the signature structure [19]. For example, to find the total amplitude, T, for the type II diagram with

Table 1
The weights for the double Regge exchange diagrams, (A)–(F) of fig. 3, for $K^{\pm}p \to K^0\pi^{\pm}p$

Quark diagram	Weight	Weight for (α_1, α_2) exchange			
Type I		(A_2, f)	(ρ, f)	(A_2, ω)	(ρ, ω)
K^-: (A) + (B)	$1 + C_1C_2$	2	0	0	2
K^+: (D) + (E)	$C_1 + C_2$	2	0	0	−2
Type II		(K_T, f)	(K_V, f)	(K_T, ω)	(K_V, ω)
K^-: (C)	C_1	1	−1	1	−1
K^+: (F)	C_1C_2	1	−1	−1	1

C_i is the charge parity of the exchange trajectory α_i. Note that β_0 of subsect. 2.2 corresponds to the (ρ, ω) contribution, $2T^{--}$, to $\bar{K}^0\pi^-$ production.

an incident K^-, we need to sum over the four Regge terms

$$T = \sum_{\alpha_1,\alpha_2} C_1 A_{\alpha_1\alpha_2} = \sum_{\alpha_1,\alpha_2} \tau_1 A_{\alpha_1\alpha_2} , \tag{25}$$

with A_{α_1,α_2} given by eq. (24). The first equality arises because the diagram has a quark twist C_1, the second because the relevant exchanges have $C_1\tau_1 = 1$. In general therefore, T contains sixteen terms. However in the EXD limit the $A^{(i)}_{\alpha_1\alpha_2}$ are independent of α_1, α_2 and so, on summing over $\tau_1, \tau_2 = \pm 1$ in eq. (25), we are left with just the $A^{(1)}$ contributions, that is

$$T = A^{(1)} .$$

In other words, in the EXD limit we may identify a quark twist with a signature twist. Since we wish to investigate the EXD breaking of trajectories we need to use the full form. That is, we calculate the signatured amplitudes of eq. (13) and take the full sum such as eq. (25). Finally, to obtain the reaction amplitude we sum * over the type I and type II diagrams for that reaction. This corresponds to summing the exchange diagrams of fig. 2 using the weights shown in brackets.

The above procedure allows us to determine all the relevant double-exchange contributions to the $K^\pm p \to K^0\pi^\pm p$ processes. For the reaction $\pi^- p \to K^- K^0 p$ we need only a subset of these double-exchange terms, namely those with $\alpha_1 = K_V, K_T$ and $\alpha_2 = \mathbb{P}$, f, ω. Note that for $K\bar{K}$ production, K_T and K_V now contribute to diagrams of both type I and type II. These contributions can be evaluated using a similar procedure to that described above for the $K\pi$ production reactions.

We note that the coupling calculation concerns only the leading vector/tensor Regge poles. We have assumed magic mixing for the ω, and likewise for the f. We leave the inclusion of pomeron exchange to subsect. 2.3. We have neglected all isospin one (α_2) exchanges (including unnatural parity) since this is known to be a good first approximation for the equivalent on-shell processes $K^\pm p \to K^{*\pm} p$, $\pi^\pm p \to A_2^\pm p$ etc. Furthermore we consider only nucleon non-flip isoscalar couplings, since both the isoscalar helicity-flip and the isovector non-flip couplings are known to be small.

2.3. Inclusion of the pomeron

In this section we wish to determine the double-exchange amplitudes of fig. 2 with f replaced by pomeron exchange. We must therefore adopt some model for the pomeron. We use the f-dominated pomeron scheme proposed by Carlitz, Green and Zee [14] in which the SU(3) singlet pomeron is taken to couple *via* f and f′ mesons. The SU(3) breaking arises explicitly from the f, f′ mass difference. This

* Note that there are no neutral isovector exchanges, $(u\bar{u}-d\bar{d})/\sqrt{2}$, to give rise to additional minus signs from $-d\bar{d}$ exchange.

simple and plausible scheme gives good agreement with elastic scattering data. However a study [12] of the data for the reactions $\pi p \to A_2 p$, $Kp \to K^* p$, which are relevant to us, indicates that the pomeron component for these reactions is about half the strength of that for elastic scattering. We must take note of this fact when applying the scheme to the double-exchange diagrams (see sect. 3). We should add that we do not consider the alternative pomeron-f identity scheme [20] as this has difficulties in reproducing the data, particularly for these relevant meson-production reactions [21].

Motivated by the f-dominated pomeron scheme we obtain a double-exchange $(\alpha_1, \alpha_2 = \alpha_{\mathrm{IP}})$ amplitude by replacing the α_2 Regge pole in eq. (5) as follows

$$\frac{1}{J_2 - \alpha_2} \to \frac{\gamma_{\mathrm{fIP}}}{J_2 - \alpha_\mathrm{f}} \frac{B_{\mathrm{IP}}}{J_2 - \alpha_{\mathrm{IP}}} \frac{\gamma_{\mathrm{fIP}}}{J_2 - \alpha_\mathrm{f}}\,, \tag{26}$$

where for simplicity we have omitted the t_2 arguments. The middle term is the (SU(3) singlet) pomeron singularity itself. γ_{fIP} is the pomeron-pomeron-f coupling. We should add a similar f′ contribution to the first term; we will allow for this when we determine the relevant couplings. Since the lower vertex contains only non-strange quarks, only the f contributes to the third term.

Inserting the pomeron singularity, eq. (26), into the Mellin representation, *via* eq. (5), and performing the helicity integration as in subsect. 2.1 we find the $(\alpha_1, \alpha_{\mathrm{IP}})$ amplitude is, to leading order, again given by eqs. (12) and (13) with the replacements $\alpha_2(t_2) \to \alpha_{\mathrm{IP}}(t_2)$ and

$$\beta_0 \to \frac{\beta_0 (\gamma_{\mathrm{fIP}})^2 B_{\mathrm{IP}}}{(\alpha_{\mathrm{IP}}(t_2) - \alpha_\mathrm{f}(t_2))^2} \equiv \beta_{\mathrm{IP}}(t_2)\,, \tag{27}$$

where again we assume no helicity dependence of the pole residue. Note that the Steinmann constraints are still preserved.

The relevant pomeron couplings can be easily obtained from those given in table 1 for the f. We need only recall the pomeron-to-f coupling ratios for two-body reactions shown in table 2. The factor r in the table is given by

$$r(t) = \frac{\alpha_{\mathrm{IP}} - \alpha_\mathrm{f}}{\alpha_{\mathrm{IP}} - \alpha_{\mathrm{f}'}} \tag{28}$$

and accounts for the possibility of f′ coupling at the meson vertex. The departure of r from unity represents the SU(3) mass-breaking effect. The ratios of table 2 embody the result that, in the symmetry limit, the pomeron decouples from K*(890) production due to generalized charge conjugation invariance. In conclusion, we see that the pomeron couplings appropriate to the double-exchange diagrams can be obtained from the f couplings of table 1 provided that the type II diagram entries of ± 1 are replaced by $(\pm 1 + r)$. Of course, the pomeron couplings, β_{IP}, contain in addition the overall x factor of table 2.

We should note that in extending the f-dominated pomeron model to our $2 \to 3$

Table 2
The pomeron-to-f coupling ratios predicted by the f, f′ dominated pomeron model

$\pi N \to \pi N$ $\pi N \to A_2 N$	$KN \to KN$ $KN \to K^*(1420)N$	 $KN \to K^*(890)N$
x	$(1+r)x$	$(1-r)x$

Contrary to the expectations of the model there is evidence [12] to suggest x is not the same for elastic and production reactions, namely $x(\mathrm{el}) \approx 2x(\mathrm{prod})$.

body reactions we are applying the coupling scheme to a pomeron-particle-reggeon vertex, where the reggeon is either A_2 or a K^*. Moreover the original model was motivated for the imaginary part of the amplitude. For the $2 \to 3$ body application the corresponding $\pi p \to$ "A_2"p (or $Kp \to$ "K^*"p) real part is not necessarily small.

3. Application to $Kp \to K\pi p$ and $\pi p \to K\bar{K}p$ data

High-statistics spectrometer data [8–11] have recently been obtained for the reactions

$$K^- p \to \bar{K}^0 \pi^- p\,,$$

$$K^+ p \to K^0 \pi^+ p\,,$$

$$\pi^- p \to K^- K^0 p\,,$$

at a laboratory momentum of 10 GeV/c, with the dimeson system produced in the forward scattering region. These data have been analysed to determine the partial-wave dimeson production amplitudes, and the results provide a suitable testing ground for our double-exchange model.

3.1. Resumé of the results of the amplitude analyses

The $K^\pm$ initiated reactions are found [9,22] to be dominated by $K^*(1^-)$, $K^*(2^+)$, resonance production by isoscalar natural parity exchange (NPE). The t dependence of K^* resonance production for the $K^\pm$ initiated reactions show a forward turnover and exhibit a cross-over near $-t = 0.3$ (GeV/c)^2. The cross-over is more pronounced for $K^*(2^+)$ than $K^*(1^-)$ production. These features can be qualitatively described by a IP, f and ω exchange picture for the quasi two-body reactions $K^\pm p \to K^{*\pm} p$ [9]. However, the data allow not only the extraction of the resonant amplitudes, but also of the $K\pi$ partial-wave amplitudes off resonance [9]. It is the behaviour of these amplitudes which allows a novel test of double Regge exchange. Moreover, the data allow the interference between the resonant and off-resonance NPE amplitudes to be determined. In particular we have empirical knowledge of both the magnitude and phase of the P wave $K\pi$ production amplitude in an extensive $K\pi$ mass interval covering the $K^*(1420)$ resonance region, for both $K^\pm$ initiated reactions. We stress two surprising features of the behaviour of the off-resonance P wave amplitudes [9], with which to confront the double Regge exchange model. First for $M_{K\pi} \sim 1.2$ GeV we find P wave $K\pi$ production for the K^+ reaction is significantly stronger than that for the K^- reaction, whereas in the $K^*(890)$ region these P waves are of approximately equal strength. This can be seen by comparing the production amplitudes shown in fig. 4. The second surprising feature is the value of the observed phase of the P wave production amplitude in the $K^*(1420)$ region. Both $K^\pm$ data were used to extract the phases of the even- and odd-signature exchange contributions to the NPE amplitudes. After allowing for the P wave $K\pi$ decay phase, the phase of the odd-signature exchange is approximately opposite to that found in the P wave resonance region, which agreed nicely with the expectations of ω exchange for $K^\pm p \to K^*(890)^\pm p$.

Consider the reaction $\pi^- p \to K^- K^0 p$. Again the data are sufficient for a partial-wave analysis of the $K^- K^0$ production amplitude [11]. The behaviour of the resulting NPE amplitudes as a function of $K^- K^0$ mass and as a function of t are shown in figs. 4 and 5 respectively. Now G parity invariance at the meson vertex restricts the even (odd) $K^- K^0$ angular momentum states to be produced *via* $G = +1$ (-1) exchange. Thus, considering just NPE, we see that D, G ... wave $K^- K^0$ production proceeds by IP and f exchange, whereas P, F ... wave $K^- K^0$ production is due to ω exchange. This difference is apparent in the data. We see that NPE produces the even-spin states, $A_2(2^+)$ and $A_2(4^+)$, more copiously than those with odd spin, such as the $g(3^-)$. The double Regge exchanges relevant to $\pi^- p \to K^- K^0 p$ are a subset of those also necessary to describe the $K\pi$ production reactions. Thus the $K^- K^0$ data * offer a more selective test of the double-exchange model.

Since we are using known phenomenological couplings to calculate the double Regge exchange contributions we not only predict the relative behaviour of the observed partial-wave amplitudes, but also the overall normalization for the above three reactions.

3.2. *Partial-wave amplitudes*

To be specific, consider the observed process $K^+ p \to K^0 \pi^+ p$. The $K^0 \pi^+$ partial-wave production amplitudes have been extracted from the data, both as a function of t_2 $(\equiv t_{pp})$ and of s_1 $(\equiv M^2)$, where M is the mass of the $K^0 \pi^+$ system. Our aim is to explain the observed features of these amplitudes in terms of the explicit double-exchange contributions specified in sect. 2. We must therefore project our amplitude, $T(s, s_1, s_2; t_1, t_2)$, describing the process $ab \to 123$ of fig. 1, into partial-wave

* Note that, even if available, $\pi^+ p \to K^+ \bar{K}^0 p$ would not give further independent information on isoscalar NPE.

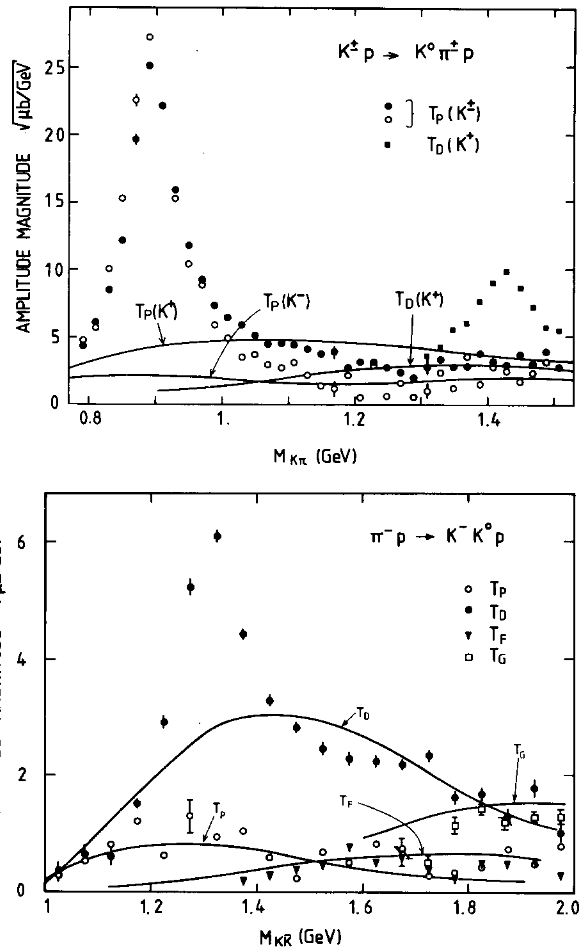

Fig. 4. The magnitudes of the dimeson partial-wave amplitudes, T_L, extracted from the data [9,11] compared with the absolute predictions of the double exchange model (shown by the curves) for (a) $K^{\pm}p \to K^0\pi^{\pm}p$, and (b) $\pi^-p \to K^-K^0p$ at 10 GeV/c. The amplitudes are normalized so that their moduli squared give the contribution to $d\sigma/dM$. The t intervals are $0.1 < -t < 0.4$ (GeV/c)^2 and $0.07 < -t < 1$ (GeV/c)^2 for (a) and (b) respectively. The D waves of the K^- induced reaction are omitted since they are almost the same as for the K^+ reaction.

amplitudes for the (12) system. We use T_L to denote the amplitude for the production of a (12) system of angular momentum L, and helicity one, by natural parity exchange. Thus

$$T_L = \sqrt{2} \int_{-1}^{1} d\cos\theta_1 \int_0^{2\pi} d\phi_1 T(s, s_1, s_2; t_1, t_2) \left[Y_L^{1*}(\theta_1, \phi_1) + Y_L^{-1*}(\theta_1, \phi_1)\right], \tag{29}$$

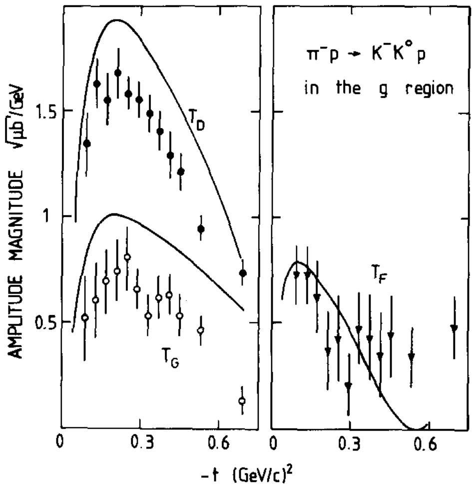

Fig. 5. The t-dependence of the 10 GeV/c $\pi^-p \to K^-K^0p$ NPE amplitudes, $|T_L|$ with $L = 2$, 3, 4 in the g region. The amplitudes are normalized so that their moduli squared give the contribution to $d\sigma/dt$. The mass interval is $1.55 < M(K^-K^0) < 1.85$ GeV. The model amplitudes shown by the curves, are absolute predictions. The data are from ref. [11].

where θ_1, ϕ_1 are the polar angles, in the (12) rest frame, specifying the direction of particle 1 with respect to the ab $\to$ (12)3 production plane. We use the t-channel helicity frame. In this frame

$$t_1 = m_1^2 + m_a^2 - 2E_aE_1 + 2p_ap_1 \cos\theta_1 ,$$

$$s_2 = m_2^2 + m_3^2 + 2E_2E_3 - 2p_2p_3(\sin\theta_1 \cos\phi_1 \sin\chi + \cos\theta_1 \cos\chi) , \qquad (30)$$

where χ is the crossing angle between the s and t channel frames describing the decay of the (12) system. Note that the full amplitude satisfies $T(2\pi - \phi) = -T(\phi)$, since $\hat{T}$ of eq. (8) depends only on $\cos\phi_1$ (*via* s_2), and the kinematical factor K is proportional to $\sin\phi_1$ (see eq. (9)). Thus we can transform to limits $(0, \pi)$ for the ϕ_1 integration.

There is a slight complication due to the occurrence of the two types of double-exchange diagrams in subsect. 2.2, namely those with a fast forward K^0 (type I) or a fast forward π^+ (type II). That is the K^0 is particle 1 (particle 2) for type I (type II). Eqs. (29) and (30) are appropriate for type I diagrams. For a type II diagram we should take $(\theta_1, \phi_1) = (\pi - \theta_K, \phi_K + \pi)$ in eq. (30) and integrate over (θ_K, ϕ_K) in eq. (29).

In order to compare our predictions with the data it is convenient to group the various double-exchange possibilities, $T_{\alpha_1\alpha_2}$, into those with $\alpha_2 = \omega$, f and IP. Thus for the reaction $K^-p \to \overline{K}^0\pi^-p$ we first form

$$T_f(\Omega_K) = 2T_{A_2f}(\Omega_K) + T_{K_Tf}(-\Omega_K) - T_{K_Vf}(-\Omega_K) ,$$

$$T_\omega(\Omega_K) = 2T_{\rho\omega}(\Omega_K) - T_{K_V\omega}(-\Omega_K) + T_{K_T\omega}(-\Omega_K) , \qquad (31a)$$

and for the f-dominated pomeron,

$$T_{\mathrm{IP}}(\Omega_{\mathrm{K}}) = 2T_{\mathrm{A_2 IP}}(\Omega_{\mathrm{K}}) + (1+r)\,T_{\mathrm{K_T IP}}(-\Omega_{\mathrm{K}}) - (1-r)\,T_{\mathrm{K_V IP}}(-\Omega_{\mathrm{K}})\,, \quad (31\mathrm{b})$$

where $\Omega_{\mathrm{K}} \equiv (\theta_{\mathrm{K}}, \phi_{\mathrm{K}})$ and $-\Omega_{\mathrm{K}} \equiv (\pi - \theta_{\mathrm{K}}, \phi_{\mathrm{K}} + \pi)$. Here we have used the weights given in tables 1 and 2. To form the amplitudes for the reactions $\mathrm{K^\pm p \to K^0 \pi^\pm p}$ we take the combinations

$$T(K^\pm) = T_{\mathrm{IP}} + T_{\mathrm{f}} \mp T_\omega\,. \quad (32)$$

We have mentioned above that the double Regge exchange contributions to the three processes are interrelated. If we use the partial-wave projections we can show the connection explicitly. For simplicity, consider the EXD and SU(3) limit. In this limit the τ_1, τ_2 exchanges satisfy

$$T^{++}(\Omega) \equiv T_{\mathrm{A_2 f}}(\Omega) = T_{\mathrm{K_T f}}(\Omega)\,,$$

$$T^{--}(\Omega) \equiv T_{\rho\omega}(\Omega) = T_{\mathrm{K_V}\omega}(\Omega)\,,$$

$$T^{+-}(\Omega) \equiv T_{\mathrm{K_T}\omega}(\Omega)\,, \qquad T^{-+}(\Omega) \equiv T_{\mathrm{K_V f}}(\Omega)\,. \quad (33)$$

Now the partial wave projection, eq. (29), satisfies

$$T_L = \sqrt{2}\int \mathrm{d}\Omega\; T(\Omega)[Y_L^1(\Omega) + Y_L^{-1}(\Omega)]^*$$

$$= (-1)^L\sqrt{2}\int \mathrm{d}\Omega\; T(-\Omega)[Y_L^1(\Omega) + Y_L^{-1}(\Omega)]^*\,.$$

Thus we can relate the type I and type II exchange contributions (*cf.* fig. 2). The results for the three reactions are given in table 3. This table emphasises the importance of comparing the model predictions for the individual partial waves, as well

Table 3
The double Regge exchange contributions, eq. (33), to the partial-wave projection of the amplitudes, defined in eq. (31), in the EXD and SU(3) limit

	$\mathrm{K^\pm p \to K^0\pi^\pm p}$		$\pi^- \mathrm{p \to K^- K^0 p}$	
	odd L	even L	odd L	even L
T_{f}	$T_L^{++} + T_L^{-+}$	$3T_L^{++} - T_L^{-+}$	0	$2T_L^{++} + 2T_L^{-+}$
T_ω	$3T_L^{--} - T_L^{+-}$	$T_L^{--} + T_L^{+-}$	$2T_L^{--} + 2T_L^{+-}$	0

L is the angular momentum of the produced dimeson system.

as for the different reactions. Moreover, due to the cancellation between type I and type II diagrams, our double-exchange model embodies the C parity selection rules for pomeron exchange, and also for K^-K^0 production.

3.3. Comparison with the data

In this subsection we compare the predictions of the double-exchange model of sect. 2 with the observed amplitudes for $K^\pm p \to K^0\pi^\pm p$ and $\pi^- p \to K^-K^0 p$ discussed in subsect. 3.1. Consider first the behaviour of the various partial-wave amplitudes as a function of the mass of the produced dimeson system. In fig. 4 we compare the NPE amplitudes, T_L, extracted directly from the data with those predicted by the exchange model. The model predictions are obtained by calculating the double Regge exchange contributions of the form of eq. (13), with $\alpha(0) = 0.5$ for ρ, ω, A_2, f and $\alpha(0) = 0.35$ for K_V and K_T. We take linear trajectories of slope $\alpha' = 0.9\ \mathrm{GeV}^{-2}$ for all reggeons. The couplings are determined as described in sect. 2.

The pomeron exchange contributions ($\alpha_1, \alpha_2 = \alpha_{\mathrm{IP}}$) can be determined, *via* factorization, in terms of the quasi-two-body reaction amplitudes for the production of resonances on the α_1 trajectory. We take the pomeron parameterization of ref. [12], which is found to give a reasonable description of these quasi-two-body processes. Though we use exactly this parametric form [12], it is equivalent, to a good approximation, to writing β_{IP} of eq. (27) in the form

$$\beta_{\mathrm{IP}} = \beta_0 \mathrm{e}^{At} x_{\mathrm{P}}/\sqrt{\pi}\ ,$$

with $t \equiv t_2$, $A = 2.5\ \mathrm{GeV}^{-2}$. As described in sect. 2 we adopt the f-f′-dominated pomeron scheme to relate β_{IP} to the normal reggeon couplings β_0, using the empirical value [12] $x_{\mathrm{P}} = 0.5$. We take $\alpha_{\mathrm{IP}} = 1 + 0.2t$.

To calculate the required partial-wave projections, T_L, we perform the integrations of eq. (29) numerically. With our normalization the cross section is

$$\frac{\mathrm{d}\sigma}{\mathrm{d}M\mathrm{d}t} = \frac{q_{12}}{128\pi p_{\mathrm{L}}^2 m_{\mathrm{N}}^2}\ \frac{1}{(2\pi)^3} \sum_L |T_L|^2 \tag{34}$$

with $t \equiv t_2$. In the figures we have renormalized the amplitudes so that their moduli squared give the contribution to $\mathrm{d}\sigma/\mathrm{d}M$ or $\mathrm{d}\sigma/\mathrm{d}t$ directly.

Recall that the model predictions have no free parameters, and that the overall normalization is determined. The comparison with the data shows that, on average, the normalization is very reasonable. Indeed, the agreement should be regarded as good considering the extrapolation necessary to estimate the exchange couplings. The observed cross section for $K\pi$ production is much larger * than for $K\bar{K}$ production. This behaviour is satisfactorily reproduced by the model. Moreover, we see that the model describes the relative magnitudes of the partial-wave amplitudes for

* This difference is more than is apparent from fig. 4, since fig. 4a corresponds to a smaller t interval than fig. 4b.

a given reaction, surprisingly well. This is support for the non-trivial double-exchange systematics, which were displayed in a simplified form in table 3.

We can only expect an exchange model approach to reproduce dimeson resonance behaviour as, at best, broad enhancements. In fact, the individual partial waves do show just such enhancements at roughly the expected mass, and moreover the double-exchange contributions conspire to give an associated resonant-type phase behaviour. This resonant behaviour is associated with the sampling of larger and larger regions of two-dimensional phase space with increasing dimeson mass. The behaviour appears analogous to the Schmid loops of 2-body scattering, but we now have different amplitude zero structure [16]. Also only one loop occurs in each partial wave and daughter states do not appear. The phases predicted by the model can be compared with the single Regge limit for $Kp \to K^*p \to K\pi p$ obtained from the same pseudoscalar dual formula using the same choice of sign of the couplings. These two predictions are in good agreement, with the exception of the odd-signature P wave. This agreement is remarkable considering that in the model we take the sum of several exchange amplitudes.

It is instructive to compare the t dependence of the data and the model for $\pi^-p \to K^-K^0p$ in the g mass region. The comparison, for the NPE amplitudes, is shown in fig. 5. Here the background partial waves, T_D and T_G, exceed the resonant wave T_F; the former arise from $\alpha_2 = \mathbb{P}$, f and the latter from $\alpha_2 = \omega$. Again, we see that the magnitudes of the partial waves, and also their t_2 dependence, are in striking agreement with the double-exchange picture. The forward turnover is due to the kinematic factor, $K \propto \sin\theta_1 \sin\phi_1$, but the remaining $t_2 \equiv t_{pp}$ dependence of the model is non-trivial. In addition to the $\alpha_2(t_2)$ dependence, we note that the s_2 and t_1 integration region increases with increasing $-t_2$. This leads, for example, to a flatter t_2 dependence for T_G than T_D, in agreement with the data.

Let us compare the behaviour of the P wave $K\pi$ amplitudes for the $K^\pm$ initiated reactions in more detail. First consider the mass behaviour shown in fig. 4. The double Regge exchange model predicts T_P for the K^+ reaction to be larger than for the K^- reaction, particularly for $M \approx 1.2$ GeV. The data do show evidence of a similar trend, but the occurrence of the K*(890) resonance makes it difficult to assess the level of agreement with the exchange model prediction. The P-D interference manifest in the data allow the phases of the NPE P wave amplitudes to be determined in the K*(1420) mass region. These phases, together with those of the resonant D wave, are shown in fig. 6 by drawing the observed amplitudes on Argand plots. Instead of showing the individual reaction amplitudes, we plot the even- and odd-signature exchange combinations, that is $T_L(K^-) \pm T_L(K^+)$ respectively. The knowledge of these phases allows a more subtle test of the double Regge exchange picture. The model predictions, shown by the dashed lines, are seen to be in reasonable agreement with the observed amplitudes. The agreement is particularly significant for the odd-signature P wave amplitude because, as mentioned in subsect. 3.1, if the single ω exchange picture were applied to $Kp \to (K\pi)p$ we would find approximately the opposite sign [9] (shown by the dotted line on fig. 6).

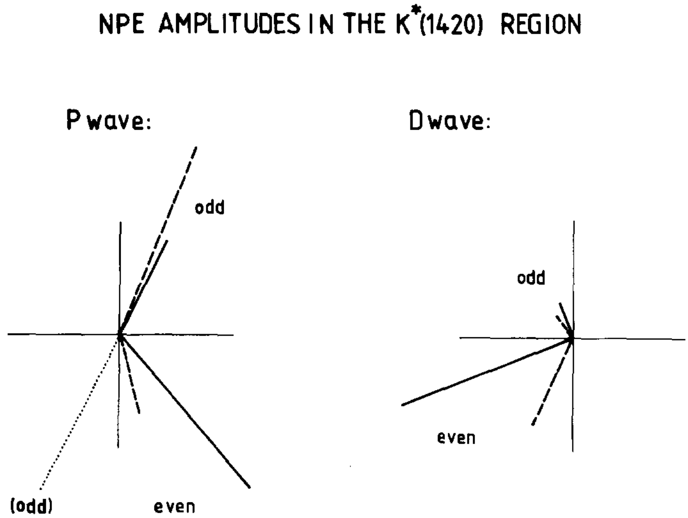

Fig. 6. The Argand diagrams for the even- and odd-signature NPE amplitudes for $K^{\pm}p \to K^0\pi^{\pm}p$ in the $K^*(1420)$ mass region and the t interval $0.1 < -t < 0.4$ $(GeV/c)^2$. We compare the P and D wave $K\pi$ amplitudes extracted from the data [11] (solid lines) with those of the model (dashed lines). To allow for mass averaging the D wave data amplitudes are plotted as half the peak values. For clarity, the P wave plot has been doubled in size relative to that for the D wave. The dotted line is a naive expectation for the odd-signature P wave phase (see text). The factor i arising from the square brackets of eq. (29) is omitted from both the data and model predictions.

Finally, we should mention that our approach is very different to a study of the same set of reactions made several years ago [23] using a crossing symmetric B_5 model. We use phenomenologically determined couplings to evaluate double-exchange contributions and so are able to make absolute predictions for both the magnitudes and phases of the amplitudes. Our only use of B_5 is in the extrapolation required to estimate the reggeon-reggeon-particle coupling. By necessity, the pomeron contributions were ignored in ref. [23]; since then it has been recognized that pomeron exchange makes a major contribution. We have compared our predictions for $K\pi$ and $K\bar{K}$ production at $p_L = 10$ GeV/c. However, if we evaluate the double-exchange model at lower momenta we find the (kinematic) enhancement of $K\pi$ production (roughly a factor of 10 above $K\bar{K}$ production) as also occurs in ref. [23].

4. Conclusions

We have described how one may make absolute predictions for the double Regge limit of high-energy processes involving three-body final states. The amplitudes were shown to have the correct analytic and factorization properties and yet be in a form suitable for comparison with experimental data. We demonstrated how to link together the various double-exchange contributions to a given reaction amplitude, and how to evaluate these contributions in terms of known coupling constants. In particular, we showed how an f-dominated pomeron singularity could be incorporated.

Ideally, one should compare with $2 \to 3$ body reaction data which is truly in the double Regge kinematical region, say $s_1, s_2 > 5-10$ GeV^2. In practice, the majority of data, even at high beam energy, occurs dominantly in the resonance region of s_1 or s_2. The $Kp \to K\pi p$ and $\pi p \to \bar{K}Kp$ data, with which we have compared, are no exception. However, we have seen that there are compensations in that one has access to more detailed information in this region (the behaviour of individual partial-wave amplitudes, interference phases, and the relation to single Regge exchange resonance production amplitudes).

Clearly, we should not expect a double-exchange approach to give detailed agreement with the empirical reaction amplitudes in the resonance region. Rather, we have investigated whether double-exchange calculations can be used to give a meaningful estimate of the average strength of a $2 \to 3$ body reaction. It is important to recall that, since we used known couplings, there are no free parameters. Our conclusion is that, just as in two-body scattering, one can use dual-model inspired Regge residues to obtain absolute predictions for the overall strength of a $2 \to 3$ body process by pole extrapolation. We found the level of agreement with data is as good as in the two-body case.

In carrying out these calculations we showed how to evaluate and how, using quark counting rules, to interrelate the double-exchange contributions. We included two types of exchange diagrams, namely types I and II, which are distinguished by which of the two produced mesons is the fast forward particle. Although a given $2 \to 3$ body reaction amplitude is the sum over many such exchange contributions, the empirical knowledge of the partial-wave amplitudes for each of the three related reactions ($K^{\pm}p \to K^0\pi^{\pm}p$, $\pi^-p \to K^-K^0p$) allowed a more selective and detailed study.

The double-exchange model is found to reproduce some of the more subtle mass and t dependent experimental features of these diffractively produced dimeson systems. In particular, the relative P, D, F, G ... wave production strengths; and the relative magnitudes and phases observed in the K^+ and K^- initiated reactions. We found the relative strength of pomeron and Regge exchange is correctly predicted by the model, which relates it to that in on-shell resonance production. The model also gives a reasonable simultaneous description of the observed features of $\pi p \to \bar{K}Kp$ and $Kp \to K\pi p$ reactions. This not only tests the SU(3) and EXD relations between the Regge residues, but also the SU(3) structure of the f-dominated pomeron amplitudes.

Although such an exchange model should not be judged by comparison with resonance production amplitudes, it is interesting to note that the partial-wave projection of the double-exchange reaction amplitudes reveal resonant-type behaviour in both magnitude and phase. These correspond well to the observed dimeson resonances, except that they are broader. Surprisingly, with one exception, the phase predicted by the model is in agreement with the quasi-two-body prediction, that is with the sum of the single Regge K^* production phase and the resonant decay phase.

We conclude that the double-exchange model should give meaningful absolute estimates of $2 \to 3$ body reaction amplitudes for arbitrary final state kinematics at high beam energies. In addition to its phenomenological and theoretical interest, we note that predictions from the model may be valuable in performing acceptance calculations for future experiments.

We wish to thank Peter Collins and David Webber for useful discussions during the course of this work, and to acknowledge the support of the Science Research Council.

References

[1] R.C. Brower, C.E. DeTar and J.H. Weis, Phys. Reports 14 (1974) 257.
[2] H.D.I. Abarbanel, Rev. Mod. Phys. 48 (1976) 417.
[3] G.C. Fox and C. Quigg, Ann. Rev. Nucl. Sci. 23 (1973) 219.
[4] A.C. Irving and R.P. Worden, Phys. Reports 34 (1977) 117.
[5] E.L. Berger, Proc. Daresbury study weekend no. 8 (1975) p. 35.
[6] G.C. Fox and A.J.G. Hey, Nucl. Phys. B56 (1973) 386.
[7] K. Bardakci and H. Ruegg, Phys. Lett. 28B (1968) 342.
[8] R. Baldi et al., Nucl. Phys. B134 (1978) 365.
[9] A.D. Martin et al., Nucl. Phys. B134 (1978) 392.
[10] R. Baldi et al., Phys. Lett. 74B (1978) 413.
[11] A.D. Martin et al., Phys. Lett. 74B (1978) 417;
A.D. Martin et al., Nucl. Phys. B140 (1978) 158.
[12] A.C. Irving, Nucl. Phys. B121 (1977) 176.
[13] P.D.B. Collins, F.D. Gault and A.D.M. Wright, J. Phys. G4 (1978) 471.
[14] R. Carlitz, M.B. Green and A. Zee, Phys. Rev. Lett. 26 (1971) 1515; Phys. Rev. D4 (1971) 3439.
[15] E.L. Berger, *in* Phenomenology in particle physics, Proc. Cal. Tech. Conf. (1971) p.83.
[16] E.L. Berger and J. Vergeest, Nucl. Phys. B116 (1977) 317.
[17] A.D. Martin, C. Michael and R.J.N. Phillips, Nucl. Phys. B43 (1972) 13.
[18] H. Pilkuhn, The interactions of hadrons (North-Holland, Amsterdam, 1967).
[19] Y. Eylon, Phys. Rev. D13 (1976) 3317; Nucl. Phys. B132 (1978) 65.
[20] G.F. Chew and C. Rosenzweig, Phys. Lett. 58B (1975) 93; Phys. Rev. D12 (1975) 3907.
[21] D.W. Duke, Phys. Lett. 71B (1977) 342;
C.-I. Tan, D.W. Tow and J. Tran Thanh Van, Phys. Lett. 74B (1978) 115.
[22] R. Baldi et al., Phys. Lett. 70B (1977) 377;
P. Estabrooks et al., Phys. Rev. D17 (1978) 658.
[23] H.M. Chan, R.O. Raitio, G.H. Thomas and N.A. Tornqvist, Nucl. Phys. B19 (1970) 173.